Theory of the Propagation of UHF Radio Waves in Coal Mine Tunnels

ALFRED G. EMSLIE, ROBERT L. LAGACE, MEMBER, IEEE, AND PETER F. STRONG

Abstract—**The theoretical study of UHF radio communication in coal mines, with particular reference to the rate of loss of signal strength along a tunnel, and from one tunnel to another around a corner is the concern of this paper. Of prime interest are the nature of the propagation mechanism and the prediction of the radio frequency that propagates with the smallest loss. The theoretical results are compared with published measurements. This work was part of an investigation of new ways to reach and extend two-way communications to the key individuals who are highly mobile within the sections and haulageways of coal mines.**

INTRODUCTION

AT FREQUENCIES in the range of 200–4000 MHz the rock and coal bounding a coal mine tunnel act as relatively low-loss dielectrics with dielectric constants in the range 5–10. Under these conditions a reasonable hypothesis is that transmission takes the form of waveguide propagation in a tunnel, since the wavelengths of the UHF waves are smaller than the tunnel dimensions. An electromagnetic wave traveling along a rectangular tunnel in a dielectric medium can propagate in any one of a number of allowed waveguide modes. All of these modes are "lossy modes" owing to the fact that any part of the wave that impinges on a wall of the tunnel is partially refracted into the surrounding dielectric and partially reflected back into the waveguide. The refracted part propagates away from the waveguide and represents a power loss. It is to be noted that the attenuation rates of the waveguide modes studied in this paper depend almost entirely on refraction loss, both for the dominant mode and higher modes excited by scattering, rather than on ohmic loss. The effect of ohmic loss due to the small conductivity of the surrounding material is found to be negligible at the frequencies of interest here (see Appendix B).

The study reported here is concerned with tunnels of rectangular cross section and the theory includes the case where the dielectric constant of the material on the side walls of the tunnel is different from that on top and bottom walls. The work, which has previously been reported [1] in summary form, extends the earlier theoretical work by Marcatili and Schmeltzer [2] and by Glaser [3], which applies to waveguides of circular and parallel-plate geometry in a medium of uniform dielectric constant. We present in the body of the paper the main features of the propagation of UHF waves in tunnels. Details of the derivations are contained in the accompanying appendices.

Manuscript received May 9, 1974; revised November 14, 1974. This work was supported by the U. S. Bureau of Mines, Pittsburgh Mining and Safety Research Center, USBM Contract H0122026. The views and conclusions contained in this document are those of the authors and should not be interpreted as necessarily representing the official policies of the Interior Department's Bureau of Mines or the U. S. Government.

The authors are with Arthur D. Little, Inc., Cambridge, Mass. 02140.

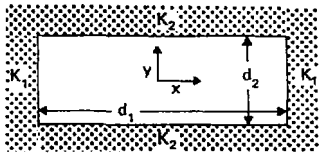

Fig. 1. Wave guide geometry.

THE FUNDAMENTAL (1,1) WAVEGUIDE MODES

The propagation modes with the lowest attenuation rates in a rectangular tunnel in a dielectric medium are the two (1,1) modes, which have the electric field $\boldsymbol{E}$ polarized predominantly in the horizontal and vertical directions, respectively. We will refer to these two modes as the E_h and E_v modes.

The main field components of the E_h mode in the tunnel are

$$E_x = E_0 \cos k_1 x \cos k_2 y \exp(-ik_3 z) \tag{1}$$

$$H_y = \frac{k_3}{\omega\mu_0} E_0 \cos k_1 x \cos k_2 y \exp(-ik_3 z) \tag{2}$$

where the symbols have their customary meaning. The coordinate system is centered in the tunnel with x horizontal, y vertical, and z along the tunnel as shown in Fig. 1. In addition to these transverse field components there are small longitudinal components of E_z and H_z and a small transverse component H_x. For the frequencies of interest here k_1 and k_2 are small compared with k_3, which means that the wave propagation is mostly in the z direction. From a geometrical optics point of view, the ray makes small grazing angles with the tunnel walls.

In the dielectric surrounding the tunnel the wave solution has the form of progressive waves in the transverse as well as the longitudinal directions. The propagation constant k_3 for the (1,1) mode is an eigenvalue determined by the boundary conditions of continuity of the tangential components of $\boldsymbol{E}$ and $\boldsymbol{H}$ at the walls of the tunnel. Owing to the simple form of the wave given by (1) and (2) these conditions can be satisfied only approximately. However,

a good approximation to k_3 is obtained. The imaginary part of k_3, which arises owing to the leaky nature of the mode, gives the attenuation rate of the wave. The loss L_{Eh} in dB for the (1,1) E_h mode is given by

$$L_{Eh} = 4.343\lambda^2 z \left(\frac{K_1}{d_1^3 (K_1 - 1)^{1/2}} + \frac{1}{d_2^3 (K_2 - 1)^{1/2}} \right) \quad (3)$$

where K_1 is the dielectric constant of the side walls and K_2 of the roof and floor of the tunnel. The corresponding result for the (1,1) E_v mode is

$$L_{Ev} = 4.343\lambda^2 z \left(\frac{1}{d_1^3 (K_1 - 1)^{1/2}} + \frac{K_2}{d_2^3 (K_2 - 1)^{1/2}} \right). \quad (4)$$

The derivation of (3) and (4), along with the generalized expressions for higher modes, is given in Appendix A, which also gives the range of validity of the formulas. The losses calculated by (3) and (4) agree closely with those calculated by a ray approach (see Appendix C).

Fig. 2 shows loss rates in dB/100 ft as functions of frequency calculated by (3) and (4) for the (1,1) E_h and E_v modes in a tunnel of width 14 ft and height 7 ft, representative of a haulageway in a seam of high coal, and for $K_1 = K_2 = 10$, corresponding to coal on all the walls of the tunnel. It is seen that the loss rate is much greater for the E_v mode. Fig. 3 shows the calculated E_h loss rate for a tunnel of half the height. The higher loss rate in the low coal tunnel is due to the effect of the d_2^3 term in (3).

Measurements of attenuation in straight coal mine tunnels, and also around corners into cross tunnels, have been made by Goddard [4][1] at frequencies of 200, 415, and 1000 MHz for various orientations of the transmitting and receiving dipole antennas. A striking feature of the results is that for 415 and 1000 MHz the rate of decay of signal strength in a straight tunnel (in dB/100 ft) is the same, within experimental error, for all orientations of the two antennas, i.e., horizontal–horizontal, vertical–horizontal, and vertical–vertical. At 200 MHz, only VH and VV measurements for a few antenna separations are reported and the decay rates are somewhat different. For comparison with the theoretical decay rates we show the experimental points on Fig. 2. The 415- and 1000-MHz points are for the HH orientation, which is almost the same as for the other orientations, while the 200-MHz point is the average of the VH and VV decay rates.

The comparison shows clearly that the propagation in the tunnel is by the (1,1) E_h mode. However, the somewhat higher values of the experimental attenuation at 415 and 1000 MHz suggest that some additional loss mechanism sets in at higher frequencies. This mechanism must also be able to account for the independence of loss rate on antenna orientation, since the theory up to this point predicts no transmission for the VH antenna arrangement.

[1] All experimental results and Fig. 4 in the present paper are taken from the work of Goddard, Collins Radio Co., Cedar Rapids, Iowa.

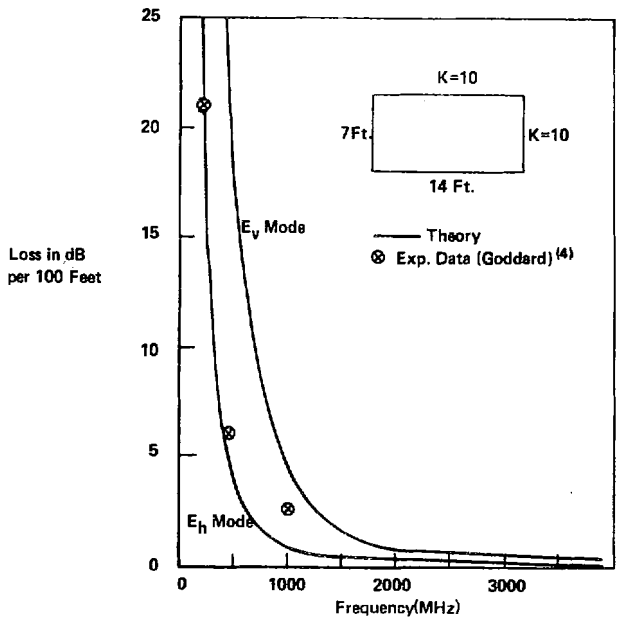

Fig. 2. Refraction loss for E_h and E_v modes in high-coal.

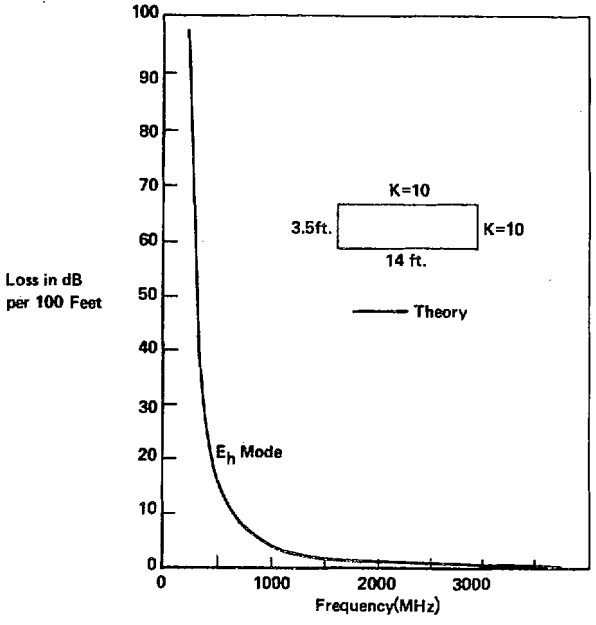

Fig. 3. Refraction loss for E_h mode in low-coal.

PROPAGATION MODEL

The higher observed loss rate at the higher frequencies relative to the calculated E_h mode values, and the independence of the loss rate on antenna orientation can both be accounted for if one allows for scattering of the dominant (1,1) E_h mode power by roughness and tilt of the tunnel walls. The scattered power goes into many higher modes and can be regarded as a "diffuse" radiation component that accompanies the E_h mode. This diffuse radiation component is in dynamical equilibrium with the E_h mode in the sense that its rate of generation by scattering of the E_h mode is balanced by its rate of loss by refraction into the surrounding dielectric. Since the diffuse compo-

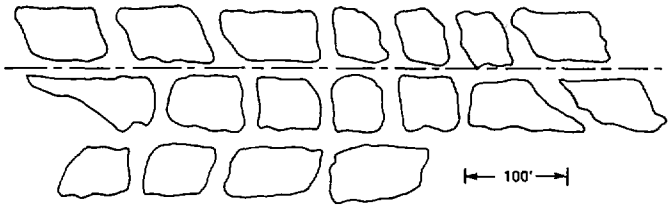

Fig. 4. Example of coal mine tunnels and cross cuts.

nent consists of contributions from the (1,1) E_v mode and many higher order waveguide modes, all of which have much higher refractive loss rates than the fundamental E_h mode, the dynamical balance point is such that the level of the diffuse component is many dB below that of the E_h mode at any point in the tunnel.

Our propagation model, comprising the (1,1) E_h mode plus an equilibrium diffuse component, explains the discrepancy between theory and experiment in Fig. 2, since the loss due to scattering of the E_h mode is greater at 1000 MHz than at 415 MHz owing to the larger effect of wall tilt at the higher frequency. The model accounts for the independence of loss rate on antenna orientation, since the loss rate is always that of the E_h mode, except for initial and final transition regions, no matter what the orientations of the two antennas may be. The transition regions, however, cause different insertion losses for the different antenna orientations.

Further strong support for the theoretical model is provided by the discovery by Goddard [4] that a large loss in signal strength occurs when the receiving antenna is moved around a corner into a cross tunnel; and that the signal strength around the corner is independent of receiving antenna orientation. We interpret these findings as follows. The (1,1) E_h mode in the main tunnel consists of a highly collimated beam of radiation owing to the small ratio of wavelength to tunnel dimensions. Such a beam acts in essentially a geometrical optics way and is almost unaffected by the openings into the cross tunnel. The (1,1) mode therefore couples very weakly into the cross tunnel modes. In this respect the situation is very different from the case of crossed mono-mode metal waveguides. Furthermore if the E_h mode did couple significantly into the cross tunnel, by symmetry the radiation in the cross tunnel would also be horizontally polarized, contrary to the experimental results.

The diffuse component in the main tunnel, on the other hand, covers a wide angular range and therefore couples strongly into the cross tunnel. Moreover, since it consists of both E_h and E_v higher modes it is largely unpolarized. Therefore the fraction of the diffuse component that enters the cross tunnel is also largely unpolarized, in accord with the experimental results.

Another experimental result is that the initial attenuation rate in the cross tunnel is much higher than the rate in the main tunnel. This is also in accord with the model since the diffuse radiation component has a much larger loss rate than the E_h mode owing to its steeper angles of incidence on the tunnel walls.

THE DIFFUSE RADIATION COMPONENT

Scattering of the (1,1) E_h mode into other modes to generate the "diffuse" component occurs by two mechanisms: wall roughness and wall tilt, which coal mine tunnels exhibit to a marked degree. Fig. 4 is a plan view that depicts typical sidewall geometry of tunnels in room and pillar coal mines. The roof and floor of these tunnels also have long range tilt variations, since the tunnels are made to follow the undulations of the coal seam.

Roughness is here regarded as local variations in the level of the surface relative to the mean level of the surface of a wall. For the case of a Gaussian distribution of the surface level, defined by a root-mean-square roughness h, the loss in dB by the E_h mode is given by the formula (see Appendix D)

$$L_{\text{roughness}} = 4.343\pi^2 h^2 \lambda \left(\frac{1}{d_1^4} + \frac{1}{d_2^4}\right) z. \tag{5}$$

This is also the gain by the diffuse component due to roughness.

It may seem surprising that the loss due to roughness increases with wavelength. The reason is that, in a ray picture of a given mode, the grazing angle of the ray on the walls of the waveguide increases with wavelength. The loss varies directly with grazing angle and number of bounces per unit length, and inversely with wavelength. Increase in wavelength increases the first two factors and decreases the third. The net effect is an increase of loss with wavelength.

Long range tilt of the tunnel walls relative to the mean planes, which define the dimensions d_1 and d_2 of the tunnel, causes power in the E_h mode to be deflected away from the directions defined by the phase condition for the mode. One can calculate the average coupling factor of such deflected radiation back into the E_h mode and thereby find the loss rate due to tilt. The result in dB is (see Appendix E)

$$L_{\text{tilt}} = \frac{4.343\pi^2\theta^2 z}{\lambda} \tag{6}$$

where θ is the root mean-square tilt. Equation (6) also gives the rate at which the diffuse component gains power from the E_h mode as a result of the tilt.

It is noted from (5) and (6) that roughness is most important at low frequencies while tilt is most important at high frequencies.

Figure 5 shows the effect on the (1,1) E_h mode propagation of adding the loss rates due to roughness and tilt to the direct refraction loss given in Fig. 2. The curves are calculated for a root-mean-square roughness of 4 in and for various assumed values of θ. It is seen that a value $\theta = 1°$ gives good agreement with the experimental values. The effect of tilt is much greater than that of roughness in the frequency range of interest.

Having determined the value of θ, for the assumed value of h, we can now find the intensity ratio of the diffuse com-

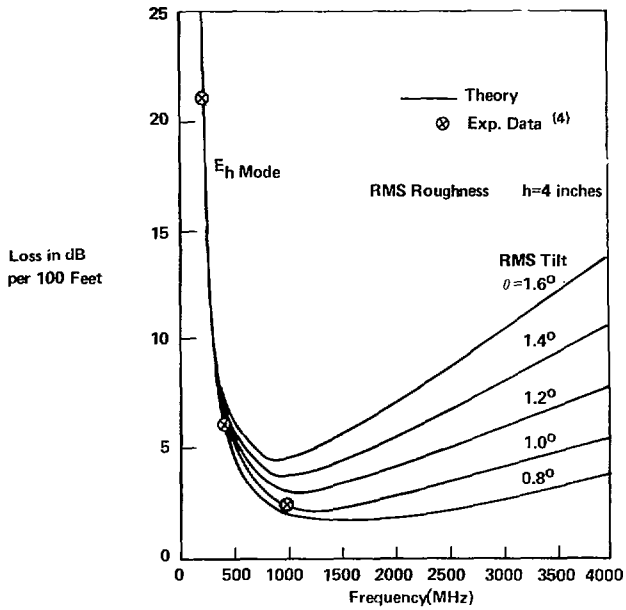

Fig. 5. Resultant propagation loss for E_h mode in high-coal (refraction, wall roughness, and tilt).

ponent to the E_h mode from the equilibrium balance equation

$$\frac{I_{d,\text{main}}}{I_{h,\text{main}}} = \frac{L_{hd}}{L_d} \tag{7}$$

where L_{hd} is the loss rate from the E_h mode into the diffuse component, and L_d is the loss rate of the diffuse component by refraction. To estimate L_d approximately, we take the loss rate to be that of an "average ray" of the diffuse component having direction cosines $(1/\sqrt{3},1/\sqrt{3},1/\sqrt{3})$. Then

$$L_d = 10\left(\frac{z}{d_1} + \frac{z}{d_2}\right)\log_{10}\frac{1}{R} \tag{8}$$

where R, the Fresnel reflectance of the average ray for $K_1 = K_2 = 10$, has the value 0.28. Then for $d_1 = 14$ ft, $d_2 = 7$ ft, $z = 100$ ft, we find that $L_d = 119$ dB/100 ft. This value has to be corrected for the loss of diffuse radiation into cross tunnels, which we assume have the same dimensions as the main tunnel and occur every 75 ft. From relative area considerations we find that this loss is 2 dB/100 ft. The corrected value is therefore

$$L_d = 121 \text{ dB/100 ft} \tag{9}$$

which is independent of frequency.

The loss rate L_{hd} is shown in Table I as a function of frequency for the 14-ft × 7-ft tunnel. The values are the sum of the roughness and tilt losses calculated by (5) and (6) for $h = 4$ in rms and $\theta = 1°$ rms. The diffuse component level relative to the E_h mode, calculated by (7), is given in the fourth column of Table I. The diffuse component is larger at high frequencies owing to the increased scattering of the E_h mode by wall tilt.

TABLE I

DIFFUSE RADIATION COMPONENT IN MAIN TUNNEL AND AT BEGINNING OF CROSS TUNNEL

f (MH_z)	λ (Ft.)	L_{hd} (dB/100 ft.)	$\frac{I_{d,\text{main}}}{I_{h,\text{main}}}$ (dB)	$\frac{I_{d,\text{cross}}}{I_{h,\text{main}}}$ (dB)
4,000	.245	5.4	-13.5	-21.7
3,000	.327	4.1	-14.7	-22.9
2,000	.49	2.8	-16.4	-24.6
1,000	.98	1.5	-19.0	-27.2
415	2.37	1.1	-20.6	-28.8
200	4.92	1.3	-19.7	-27.9

PROPAGATION AROUND A CORNER

From solid angle considerations (see Appendix F) one finds that the fraction of the diffuse component in the main tunnel that enters the 14-ft × 7-ft aperture of a cross tunnel is 15 percent or −8.2 dB. The diffuse level just inside the aperture of the cross tunnel, relative to the E_h mode level in the main tunnel is therefore obtained by subtracting 8.2 dB from the values in column 4 of Table I. The results are shown in column 5 of the table. A dipole antenna with either horizontal or vertical orientation placed at this point responds to one half of the diffuse radiation, and therefore gives a signal that is 3 dB less than the values in column 5 of Table I, relative to a horizontal antenna in the main tunnel.

If a horizontal antenna is moved down the cross tunnel the loss rate is initially 119 dB/100 ft (the value calculated here without correction for tunnels branching from the cross tunnel). Ultimately, however, the loss rate becomes that of the E_h mode excited in the cross tunnel by the diffuse radiation in the main tunnel. We determine the E_h level at the beginning of the cross tunnel by calculating the fraction of the diffuse radiation leaving the exit aperture of the main tunnel, which lies within the solid angle of acceptance of the E_h mode in the cross tunnel (see Appendix F). The result is

$$\frac{I_{h,\text{cross}}}{I_{d,\text{main}}} = \frac{\lambda^3}{16\pi d_1^2 d_2}. \tag{10}$$

This ratio, in dB, is given in column 2 of Table II.

Column 3 of Table II is the E_h level at the beginning of the cross tunnel relative to the E_h level in the main tunnel found by adding column 2 of Table II and column 4 of Table I. We find the corresponding ratio at 100 ft down the cross tunnel by adding the E_h propagation loss rates given in Fig. 3 for $\theta = 1°$. The results are shown in the last column of Table II.

The foregoing theoretical results for the diffuse and E_h components in the cross tunnel allow us to plot straight lines showing the initial and final trends in signal level in the cross tunnel. These asymptotic lines are shown in Figs. 6 and 7 for 415 MHz and 1000 MHz, in comparison with the cross tunnel measurements. The agreement both in absolute level and distance dependence gives good support to the theoretical model.

TABLE II

EXCITATION OF E_h MODE IN CROSS TUNNEL BY DIFFUSE COMPONENT IN MAIN TUNNEL

f (MHz)	$\frac{I_{h,cross}}{I_{d,main}}$ (dB)	$\left(\frac{I_{h,cross}}{I_{h,main}}\right)_0$ (dB)	$-\left(\frac{I_{h,cross}}{I_{h,main}}\right)_{100'}$ (dB)
4,000	-66.7	-80.2	85.6
3,000	-62.9	-77.6	81.8
2,000	-57.7	-74.1	77.1
1,000	-48.6	-67.6	70.1
415	-37.1	-57.7	64.1
200	-27.6	-47.3	71.6

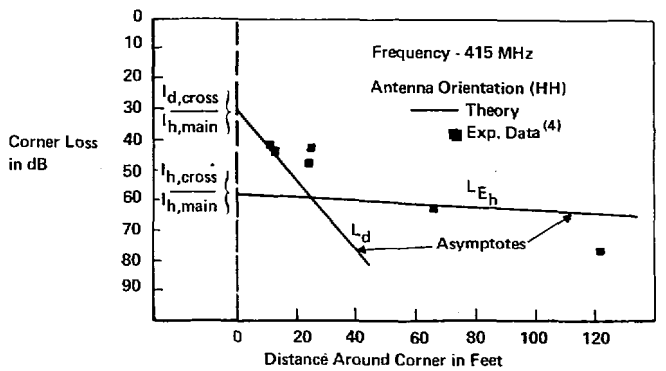

Fig. 6. Corner loss in high-coal (frequency 415 MHz).

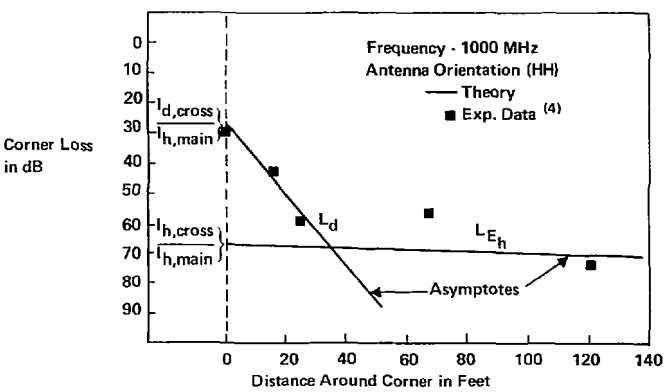

Fig. 7. Corner loss in high-coal (frequency 1000 MHz).

EFFECT OF ANTENNA ORIENTATION

The theoretical model also allows us to predict the effect of antenna orientation when the transmitting and receiving antennas are far enough apart so that dynamical equilibrium between the E_h mode and the diffuse component is established. We start with both antennas horizontal (HH configuration) and consider this as the 0-dB reference. Then if the receiving antenna is rotated to the vertical (HV configuration) this antenna is now orthogonal to the E_h mode, and therefore responds only to one half of the diffuse component, so that the loss is 3 dB more than the values in Table I, column 4. The result is shown in Table III, column 2. Now, by the principle of reciprocity, the transmission for VH is the same as for HV as shown in column 3 of Table III. We now rotate the receiving antenna to get the configuration VV. Again we incur an additional transmission loss of 3 dB more than the values

TABLE III

EFFECT OF ANTENNA ORIENTATION

f (MHz)	HH (dB)	HV (dB)	VH (dB)	VV (dB)
1000	0	-22.0	-22.0	-44.0
415	0	-23.6	-23.6	-47.2
200	0	-22.7	-22.7	-45.4

TABLE IV

INSERTION LOSS (L_i) (FOR HALF-WAVE ANTENNA)

F (MHz)	λ (Feet)	L_i (dB)
4000	0.245	35.0
3000	0.327	32.4
2000	0.49	28.9
1000	0.98	22.9
415	2.37	15.2
200	4.92	8.9

in Table I, column 4. The VV values are shown in Table III, column 4.

ANTENNA INSERTION LOSS

Dipole or whip antennas are the most convenient for portable radio communications between individuals. However, a considerable loss of signal power occurs at both the transmitter and receiver when simple dipole antennas are used because of the inefficient coupling of these antennas to the waveguide mode. The insertion loss of each dipole antenna can be calculated by a standard microwave circuit technique for computing the amount of power coupled into a waveguide mode by a probe, whereby the dipole antenna is represented as a surface current filament having a sinusoidal current distribution along its length (see Appendix G). For the E_h (1,1) mode the result for a dipole placed at the point (x_0,y_0) in the tunnel cross section is

$$C = \frac{Z_{0,1,1}\lambda^2}{\pi^2 R_r d_1 d_2} \cos^2 \frac{\pi x_0}{d_1} \cos^2 \frac{\pi y_0}{d_2}. \tag{11}$$

$Z_{0,1,1}$ is the characteristic impedance of the E_h (1,1) mode and R_r is the radiation resistance of the antenna, which are approximately the free space values 377 Ω and 73 Ω, respectively, provided that λ is small compared with d_1 and d_2.

For the case of antennas placed at the center of the tunnel ($x_0 = 0, y_0 = 0$), (11) gives the results shown in Table IV, where the insertion loss L_i in dB is equal to $-10 \log_{10} C$. It is seen that the insertion loss decreases rapidly with increasing wavelength, as one would expect, since the antenna size occupies a larger fraction of the width of the waveguide. The overall insertion loss, for both antennas, is twice the value given in the table. A considerable reduction in loss would result if high gain antenna systems were used.

OVERALL LOSS IN A STRAIGHT TUNNEL

The overall loss in signal strength in a straight tunnel is the sum of the propagation loss and the insertion losses of the transmitting and receiving antennas. Table V lists the component loss rates for the (1,1) E_h mode due to direct

TABLE V

CALCULATION OF OVERALL LOSS FOR E_h MODE WITH TWO HALF-WAVE DIPOLE ANTENNAS ($h = \frac{1}{3}$ ft, $\theta = 1°$, $K_1 = K_2 = 10$, $d_1 = 14$ ft, $d_2 = 7$ ft)

f (MHz)	$L_{refraction}$ (dB/100')	$L_{roughness}$ (dB/100')	L_{tilt} (dB/100')	$L_{propagation}$ (dB/100')	$L_{insertion}$ (dB)	$L_{overall}$ (dB) 100'	500'	1000'	1500'	2000'
4000	.06	.05	5.33	5.44	69.90	75	97	124	152	179
3000	.10	.07	3.99	4.16	64.88	69	86	107	127	148
2000	.23	.10	2.66	2.99	57.86	61	73	88	103	118
1000	.91	.21	1.33	2.45	45.82	48	58	70	81	93
415	5.34	.50	0.55	6.39	30.48	37	62	94	126	158
200	23.00	1.04	0.27	24.31	17.80	42	139	261	383	504
100	92.00	2.08	0.14	94.20	5.80	100	477	948	1419	1890

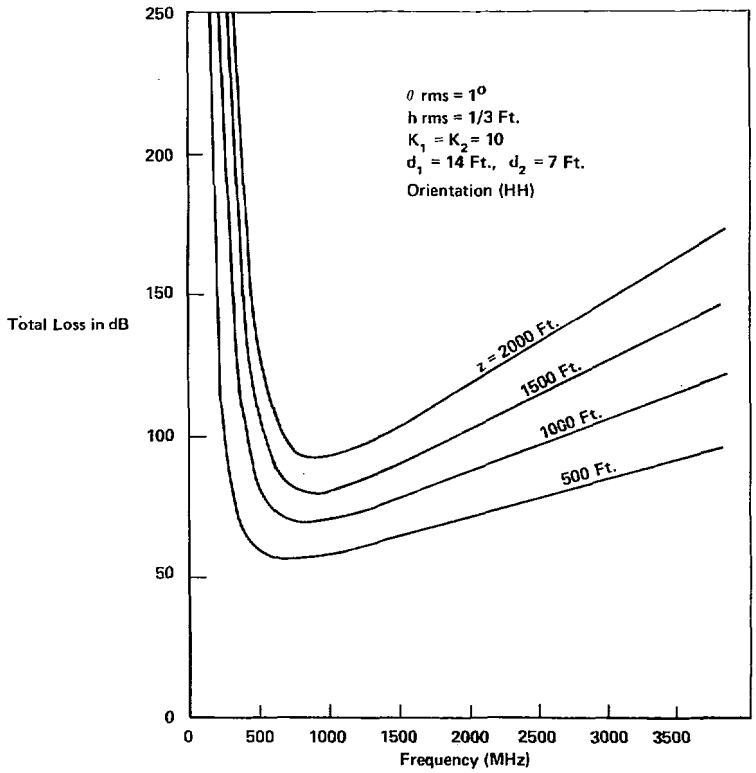

Fig. 8. Overall loss for various distances along a straight tunnel (for halfwave antennas).

refraction, roughness, and tilt; the total propagation loss rate; the insertion loss for two half-wave antennas; and the overall loss for five different distances. The overall loss for the HH orientation is also shown in Fig. 8, where it is seen that the optimum frequency for minimum overall loss is in the range 500–1000 MHz, depending on the desired communication distance.

It is also of interest to combine the results in Table V with those in Table III to obtain the overall loss versus distance for the HH, HV (or VH), and VV antenna orientations. In order to compare the theoretical values with the experimental data, which are expressed with reference to isotropic antennas, we add 4.3 dB to the overall loss calculated for half-wave dipoles. The theoretical results for the three different antenna orientations for frequencies of 415 MHz and 1000 MHz are compared with the experimental data in Figs. 9 and 10. It is seen that the theory agrees quite well with the general trend of the data.

OVERALL LOSS ALONG A PATH WITH ONE CORNER

Table VI gives the overall E_h mode loss for a path from one tunnel to another, including the corner loss involved in reestablishing the E_h mode in the second tunnel. The loss is the sum of the corner loss, given in Column 3 of Table II and repeated in Table VI, and the straight tunnel loss given in Table V for various total distances. The results in Table VI are for the case of half-wave dipole transmitting and receiving antennas and are valid when neither antenna is within about 100 ft of the corner. The overall loss is less than the values in Table VI if the receiving antenna is within this distance, owing to the presence of the rapidly attenuating diffuse component that passes around the corner. From the principle of reciprocity, the same is true if the transmitting antenna is within 100 ft of the corner.

The results indicate that the optimum frequency lies

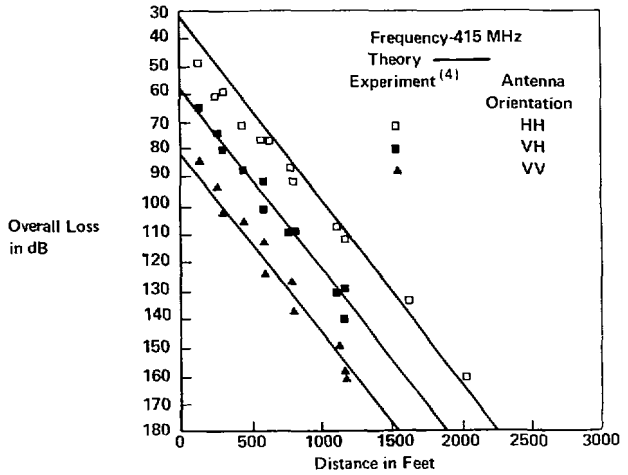

Fig. 9. Overall loss in straight tunnel in high-coal (for isotropic antennas, frequency 415 MHz).

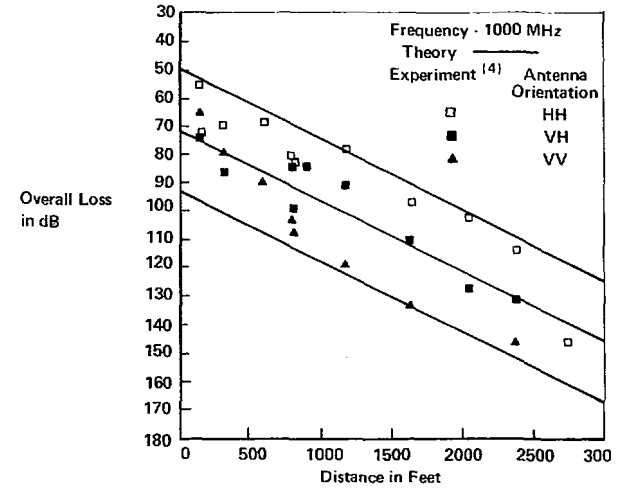

Fig. 10. Overall loss in straight tunnel in high-coal (for isotropic antennas, frequency 1000 MHz).

in the range 400–1000 MHz. However, if one installs horizontal half-wave resonant scattering dipoles with 45° azimuth in the important tunnel intersections, in order to guide the E_h mode around the corner, the optimum may shift to somewhat lower frequencies since a greater fraction of the incident E_h wave will be deflected by the longer low-frequency dipoles.

EXPECTED COMMUNICATION RANGE BETWEEN TWO ROVING MINERS

Communication can be maintained between two separated individuals until the separation distance increases to a point where the signal strength is not sufficient to overcome the background electrical noise. To obtain estimates of this communication range for a mobile application involving roving miners equipped with portable personal radio transceivers, three frequency independent loss factors should be added to the values of overall loss presented in Tables V and VI. These factors are: polarization loss-to account for likely misalignment of transmit and receive antennas; antenna efficiency

TABLE VI
OVERALL LOSS ALONG PATH INCLUDING ONE CORNER (E_h MODE WITH HALF-WAVE DIPOLE ANTENNAS)

f (MHz)	E_h Loss per Corner (dB)	Overall Loss (dB) 500′	1000′	1500′	2000′
4000	80.2	177	205	232	259
3000	77.6	163	184	205	226
2000	74.1	147	162	177	192
1000	67.6	126	138	148	161
415	57.7	120	152	184	216
200	47.3	187	308	430	551

loss-to account for the nonideal antenna installation on the portable units; and fade margin-to account for signal cancellation effects due to destructive interference. Nominal values that appear reasonable for these factors are 12 dB, 4 dB, and 12 dB, respectively, resulting in a total of 28 dB to be added to the aforementioned values of overall loss. By exercising care in the orientation and position of the portable radios in the mine tunnel cross section while communicating, these polarization and signal fading losses can of course be reduced, thereby producing a corresponding increase in range.

Representative values of receiver sensitivity and transmitter power for FM portable radios in the UHF 450-MHz band are 0.5 μV for 20 dB of quieting (-113 dBm into a 50-Ω input resistance) and 2 W (33 dBm), respectively, resulting in a total allowable loss of 146 dB. In this frequency band, measurements in mines have shown that the intrinsic electrical noise of the UHF receiver will predominate over externally generated mine electrical noise. Using the aforementioned parameter values in conjunction with the 415-MHz overall loss values presented in Tables V and VI for straight line transmission paths and paths including one corner, predictions of communication range along haulageways and in working sections of mines can be obtained, as shown in Fig. 11. Fig. 11 illustrates the coverage expected in a high-coal mine between a centrally located miner with a portable radio and a second miner roving throughout a typical 600- $\times$ 600-ft room and pillar mine section with another portable unit at an operating frequency of 415 MHz.

When the signal must go around only one corner, satisfactory communication can be expected over a linear distance of approximately 500 ft down an entry and cross-cut. When no corners are encountered, as in a haulageway transmission path, satisfactory straight line communication can be expected over distances in excess of 1500 ft. These range limits are somewhat conservative estimates, and as mentioned, can usually be somewhat extended if the portables are rotated into the horizontal plane, pointed across the tunnel, and translated a little to a more favorable signal strength position, thereby taking full advantage of the dominant horizontal field component and minimizing destructive interference effects.

Wireless coverage has been estimated using the 415-MHz frequency results because the 450-MHz UHF frequency band is the present upper limit for commercially available portable radio transceivers, and because operating frequencies near 400 MHz are most favorable for

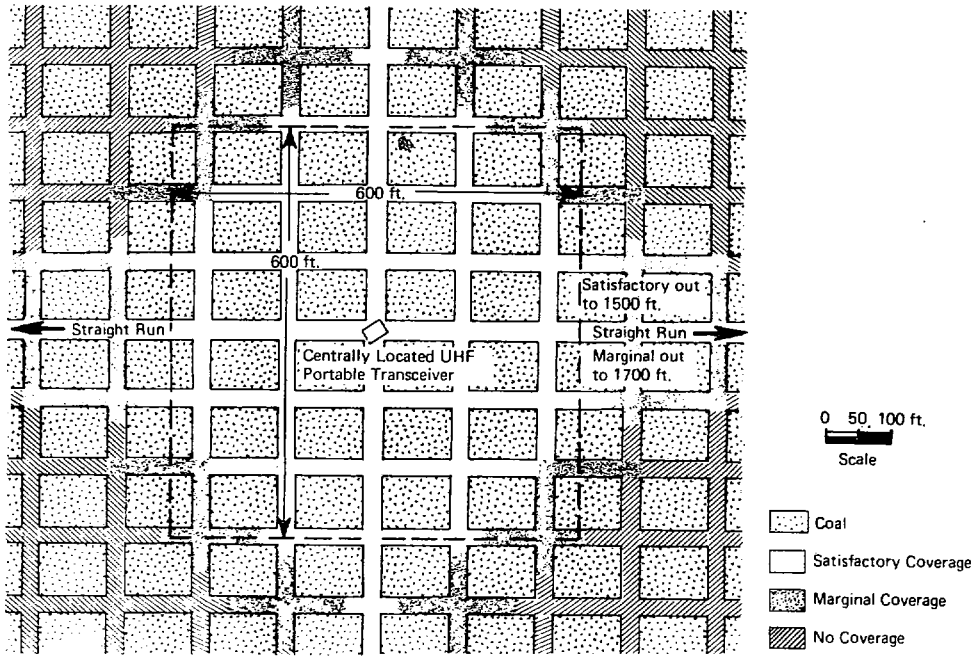

Fig. 11. Predicted UHF wireless radio coverage for 2-W portable radios in high-(7-ft) coal mine section, frequency 415 MHz.

U.S. high-coal room and pillar section applications where transmission paths typically include one corner.[2]

CONCLUSIONS

The kind of propagation model developed in this paper, involving the (1,1) E_h waveguide mode accompanied by a "diffuse" component in dynamical equilibrium with it seems to be necessary to account for the many effects observed in the measurements of Goddard [4]: the exponential decay of the wave; the marked polarization effects in a straight tunnel; the independence of decay rate on antenna orientation; the absence of polarization at the beginning of a cross tunnel; the two-slope decay characteristic in a cross tunnel; and overall frequency dependence. All of these effects are moderately well accounted for by the theoretical model. However, considerable refinement of the theory could be made by removing some of the present oversimplifications, such as the assumption of perfectly diffuse scattering both in the main tunnel and immediately around a corner in a cross tunnel, the use of the "average ray" approximation, and the description of the propagation around a corner in terms of two asymptotes only. More data at greater distances down a cross tunnel and data covering a wider frequency range in both main and cross tunnels would allow a more stringent test of the theory.

[2] Additional information regarding the practical application of UHF wireless radio systems to mine haulageways and sections is given in a paper coauthored by R. Lagace of Arthur D. Little, Inc., and H. Parkinson of the U. S. Bureau of Mines, Pittsburgh Mining and Safety Research Center, entitled "Two-way communications with roving miners," and published in U. S. Bureau of Mines Information Circular 8635, "Mine Communications" [5].

ACKNOWLEDGMENT

The authors wish to thank H. Parkinson of the U. S. Bureau of Mines, Pittsburgh Mining and Safety Research Center for his encouragement and support of this work, and A. Goddard and D. Anderson of Collins Radio Co., Cedar Rapids, Iowa, for their cooperation in supplying and discussing their experimental data prior to its publication.

APPENDIX A

MODE CALCULATIONS

A. (1,1) E_h and E_v Modes

The fundamental (1,1) E_h mode is approximately a TEM wave given by (1) and (2). The complete field of this form in the tunnel ($-d_1/2 \leq x \leq d_1/2, -d_2/2 \leq y \leq d_2/2$), satisfying Maxwell's equations, is

$$E_x = E_0 \cos k_1 x \cos k_2 y \exp(-ik_3 z) \tag{A1}$$

$$E_y = 0 \tag{A2}$$

$$E_z = \frac{ik_1}{k_3} E_0 \sin k_1 x \cos k_2 y \exp(-ik_3 z) \tag{A3}$$

$$H_x = \frac{k_1 k_2}{\omega \mu_0 k_3} E_0 \sin k_1 x \sin k_2 y \exp(-ik_3 z) \tag{A4}$$

$$H_y = \frac{(k_1^2 + k_3^2)}{\omega \mu_0 k_3} E_0 \cos k_1 x \cos k_2 y \exp(-ik_3 z) \tag{A5}$$

$$H_z = \frac{ik_2}{\omega \mu_0} E_0 \cos k_1 x \sin k_2 y \exp(-ik_3 z) \tag{A6}$$

where

$$k_1^2 + k_2^2 + k_3^2 = k_0^2 = \frac{4\pi^2}{\lambda^2}. \tag{A7}$$

Since the wavelengths of interest are small compared with the tunnel dimensions, the wave vector components k_1 and k_2 are small compared with k_3, which is close to $k_0 = 2\pi/\lambda$. Therefore H_y reduces to the expression given in (2) and E_z, H_x, and H_z are very small.

In the roof ($y \geq d_2/2$) of dielectric constant K_2, the field must represent an outgoing wave in the y direction and therefore has the form

$$E_x = B \cos k_1 x \exp(-ik_2' y) \exp(-ik_3 z) \tag{A8}$$

$$E_y = 0 \tag{A9}$$

$$E_z = \frac{ik_1}{k_3} B \sin k_1 x \exp(-ik_2' y) \exp(-ik_3 z) \tag{A10}$$

$$H_x = \frac{ik_1 k_2'}{\omega\mu_0 k_3} B \sin k_1 x \exp(-ik_2' y) \exp(-ik_3 z) \tag{A11}$$

$$H_y = \frac{(k_3^2 + k_1^2)}{\omega\mu_0 k_3} B \cos k_1 x \exp(-ik_2' y) \exp(-ik_3 z) \tag{A12}$$

$$H_z = -\frac{k_2'}{\omega\mu_0} B \cos k_1 x \exp(-ik_2' y) \exp(-ik_3 z) \tag{A13}$$

which satisfies Maxwell's equations. The wave number component k_2' in the dielectric is given by the relation

$$k_1^2 + k_2'^2 + k_3^2 = K_2 k_0^2. \tag{A14}$$

The boundary conditions at $y = d_2/2$ are that the tangential components of E and H are continuous. These conditions require that

$$E_0 \cos\left(\frac{k_2 d_2}{2}\right) = B \exp\left(\frac{-ik_2' d_2}{2}\right) \tag{A15}$$

and

$$k_2 E_0 \sin\left(\frac{k_2 d_2}{2}\right) = ik_2' B \exp\left(\frac{-ik_2' d_2}{2}\right) \tag{A16}$$

from which we obtain the condition

$$k_2 \tan\frac{k_2 d_2}{2} = ik_2'. \tag{A17}$$

Since k_1 and k_2 are small compared with k_0 we find from (A7) and (A14) that k_2' is given approximately by

$$k_2' = k_0(K_2 - 1)^{1/2}. \tag{A18}$$

Therefore, from (A17) and (A18) we obtain the following mode condition for k_2, for modes that are even functions of y:

$$k_2 \tan\frac{k_2 d_2}{2} = ik_0(K_2 - 1)^{1/2}. \tag{A19}$$

This equation could readily be solved numerically for the eigenvalues of k_2, for given values of the other quantities. However, we prefer here to obtain an approximate closed form expression that provides a better insight into the problem.

Since $k_2 d_2/2 \ll 1$ we find for the lowest E_h mode

$$k_2 \cong \frac{\pi}{d_2} + \frac{i\lambda}{d_2^2(K_2 - 1)^{1/2}}. \tag{A20}$$

This result shows that, except for a small imaginary part, k_2 has the same value as for a metal waveguide. The imaginary part arises from the power loss due to the outgoing refracted wave. The approximation involved in (A20) is valid provided that λ is small compared with $\pi d_2(K_2 - 1)^{1/2}$. This criterion is very well satisfied, for example, for $\lambda = 1$ ft, $d_2 = 7$ ft, $K_2 = 10$.

In the side wall ($x \geq d_1/2$), of dielectric constant K_1, the field has the form

$$E_x = A \exp(-ik_1' x) \cos k_2 y \exp(-ik_3 z) \tag{A21}$$

$$E_y = 0 \tag{A22}$$

$$E_z = -\frac{k_1'}{k_3} \exp(-ik_1' x) \cos k_2 y \exp(-ik_3 z) \tag{A23}$$

$$H_x = \frac{ik_1' k_2}{\omega\mu_0 k_3} A \exp(-ik_1' x) \cos k_2 y \exp(-ik_3 z) \tag{A24}$$

$$H_y = \frac{(k_1'^2 + k_3^2)}{\omega\mu_0 k_3} A \exp(-ik_1' x) \cos k_2 y \exp(-ik_3 z) \tag{A25}$$

$$H_z = \frac{ik_2}{\omega\mu_0} A \exp(-ik_1' x) \sin k_2 y \exp(-ik_3 z) \tag{A26}$$

where

$$k_1'^2 + k_2^2 + k_3^2 = K_1 k_0^2. \tag{A27}$$

Continuity of the tangential E-field gives the condition

$$k_1 E_0 \sin\left(\frac{k_1 d_1}{2}\right) = ik_1' A \exp\left(\frac{-ik_1' d_1}{2}\right). \tag{A28}$$

Continuity of H_y and H_z requires that

$$(k_3^2 + k_1^2) E_0 \cos\left(\frac{k_1 d_1}{2}\right) = (k_3^2 + k_1'^2) A \exp\left(\frac{-ik_1' d_1}{2}\right) \tag{A29}$$

and

$$k_2 E_0 \cos\left(\frac{k_1 d_1}{2}\right) = k_2 A \exp\left(\frac{-ik_1' d_1}{2}\right). \tag{A30}$$

Since (A29) and (A30) are inconsistent we can only satisfy the H boundary condition approximately. We note that since $K_1 \gg 1$, $|k_1'|$ is of the same order as k_0, whereas $|k_2|$ is much smaller. Therefore we may ignore (A30) and

TABLE VII
LOSS RATES FOR VARIOUS MODES

n_1	n_2	L_{Eh} (dB/100 ft)	L_{Ev} (dB/100 ft)
1	1	0.9	4.1
1	2	2.1	16.3
2	1	2.4	4.3
2	2	3.6	16.4
1	3	4.2	36.5
3	1	5.0	5.0
2	3	5.7	36.7
3	2	6.2	16.7
3	3	8.2	36.9

also, from (A7) and (A27), write

$$k_1^2 + k_3^2 \approx k_0^2 \tag{A31}$$

$$k_1'^2 + k_3^2 \approx K_1 k_0^2. \tag{A32}$$

Then from (A28), (A29), (A31), and (A32) we obtain, approximately,

$$k_1 \tan\left(\frac{k_1 d_1}{2}\right) = \frac{ik_0(K_1 - 1)^{1/2}}{K_1}. \tag{A33}$$

Again taking advantage of the smallness of k_1 and k_2 relative to k_0, we find for the lowest E_h mode that

$$k_1 \cong \frac{\pi}{d_1} + \frac{iK_1\lambda}{d_1^2(K_1 - 1)^{1/2}} \tag{A34}$$

which shows that the mode shape in the x direction is also the same as for a metal waveguide, except for a small imaginary part. The approximation is valid if λ is small compared with $\pi d_1(K_1 - 1/K_1)^{1/2}$. The criterion is well satisfied for $\lambda = 1$ ft, $d_1 = 14$ ft, $K_1 = 10$.

On substituting for k_1 and k_2 from (A34) and (A20) into (A7) we find, on neglecting second-order terms, that the propagation constant in the z direction is

$$k_3 = k_0 - \frac{i\lambda^2}{2}\left(\frac{K_1}{d_1^3(K_1 - 1)^{1/2}} + \frac{1}{d_2^3(K_2 - 1)^{1/2}}\right). \tag{A35}$$

The power loss in dB for the (1,1) E_h mode for a distance z is therefore

$$L_{Eh} = -8.686 \text{ Im } (k_3)$$

$$= 4.343\lambda^2 z\left(\frac{K_1}{d_1^3(K_1 - 1)^{1/2}} + \frac{1}{d_2^3(K_2 - 1)^{1/2}}\right). \tag{A36}$$

We obtain the loss for the (1,1) E_v mode by interchanging the subscripts 1 and 2 in (A36)

$$L_{Ev} = 4.343\lambda^2 z\left(\frac{1}{d_1^3(K_1 - 1)^{1/2}} + \frac{K_2}{d_2^3(K_2 - 1)^{1/2}}\right). \tag{A37}$$

As a check on these formulas we find that exactly the same results are obtained if one adds the losses for two infinite slot waveguides of slot widths d_1, d_2 and dielectric constants K_1, K_2, respectively. The numerical results given by (A36) and (A37) also agree well with those given by the ray method (see Appendix C).

B. Higher Modes

One can readily generalize (A36) and (A37) to the case of a higher mode (n_1,n_2) with approximately n_1 half-wave loops in the x direction and n_2 in the y direction. The results are

$$L_{Eh}(n_1,n_2) = 4.343\lambda^2 z\left(\frac{n_1^2 K_1}{d_1^3(K_1 - 1)^{1/2}} + \frac{n_2^2}{d_2^3(K_2 - 1)^{1/2}}\right) \tag{A38}$$

$$L_{Ev}(n_1,n_2) = 4.343\lambda^2 z\left(\frac{n_1^2}{d_1^3(K_1 - 1)^{1/2}} + \frac{n_2^2 K_2}{d_2^3(K_2 - 1)^{1/2}}\right). \tag{A39}$$

Table VII shows the loss rates for a number of modes for $f = 1000$ MHz, $\lambda = 0.98$ ft, $d_1 = 14$ ft, $d_2 = 7$ ft., $K_1 = K_2 = 10$, $z = 100$ ft.

The validity criteria for the approximate solutions of the mode conditions (A19) and (A20) are the same as for the (1,1) modes, i.e., they do not depend on n_2 or n_1.

APPENDIX B

EFFECT OF CONDUCTIVITY ON PROPAGATION LOSS

To find the effect of the finite conductivity of the walls of the tunnel on the propagation loss we now regard K_1 and K_2 as complex numbers in the approximate solutions for the eigenvalues of k_1 and k_2, which, for the general case of an E_h mode, take the form

$$k_1 = n_1\left(\frac{\pi}{d_1} + \frac{iK_1\lambda}{d_1^2(K_1 - 1)^{1/2}}\right) \tag{B1}$$

$$k_2 = n_2\left(\frac{\pi}{d_2} + \frac{i\lambda}{d_2^2(K_2 - 1)^{1/2}}\right). \tag{B2}$$

The propagation constant k_3 is given by

$$k_3^2 = k_0^2 - k_1^2 - k_2^2. \tag{B3}$$

Since k_1 and k_2 are assumed to be small compared with k_0, we can express the power absorption coefficient α_h for E_h modes in the form

$$\alpha_h = -2 \text{ Im } (k_3) \cong \frac{1}{k_0} \text{ Im } (k_1^2 + k_2^2)$$

$$= \frac{\lambda}{2\pi} \text{ Im } (k_1^2 + k_2^2). \tag{B4}$$

On substituting for k_1 and k_2 from (B1) and (B2) into (B4) we obtain

$$\alpha_h = \lambda^2 \text{ Re}\left(\frac{n_1^2 K_1}{d_1^3(K_1 - 1)^{1/2}} + \frac{n_2^2}{d_2^3(K_2 - 1)^{1/2}}\right)$$

$$- \frac{\lambda^3}{2\pi} \text{ Im}\left(\frac{n_1^2 K_1^2}{d_1^4(K_1 - 1)} + \frac{n_2^2}{d_2^4(K_2 - 1)}\right). \tag{B5}$$

We now write K_1 and K_2 in the form

$$K_1 = K_1' - iK_1'' \tag{B6}$$

$$K_2 = K_2' - iK_2'' \tag{B7}$$

where K_1'' and K_2'' are assumed to be small compared with K_1' and K_2'. Under these conditions (B5) becomes, up to first-order terms in K_1'' and K_2''

$$\alpha_h \cong \lambda^2 \left(\frac{n_1^2 K_1'}{d_1^3 (K_1' - 1)^{1/2}} + \frac{n_2^2}{d_2^3 (K_2' - 1)^{1/2}} \right) + \frac{\lambda^3}{2\pi} \left(\frac{n_1^2 K_1' (K_1' - 2) K_1''}{d_1^4 (K_1' - 1)^2} - \frac{n_2^2 K_2''}{d_2^4 (K_2' - 1)^2} \right). \tag{B8}$$

If σ_1 and σ_2 are the conductivities of the vertical and horizontal walls of the tunnel, and f is the frequency of the radiation, then

$$K_1'' = \frac{\sigma_1}{2\pi f \epsilon_0} \tag{B9}$$

$$K_2'' = \frac{\sigma_2}{2\pi f \epsilon_0}. \tag{B10}$$

Let $\sigma_1 = \sigma_2 = 10^{-2}$ mho/m,[3] $f = 1000$ MHz, $\epsilon_0 = 8.85 \times 10^{-12}$ F/m. Then $K_1'' = K_2'' = 0.18$. For $K_1' = K_2' = 10$, $d_1 = 14$ ft, $d_2 = 7$ ft, $\lambda \simeq 1$ ft, $n_1 = n_2 = 1$, the λ^2 and λ^3 terms in (B8) are then 2.19×10^{-3} ft^{-1} and 5.89×10^{-7} ft^{-1}, respectively. Thus the effect of conductivity is completely negligible in the frequency range of interest. It is to be noted that $\tan \delta = 0.018$ for the case chosen.

The very small contribution of conductivity to the propagation loss for small values of the loss tangent of the dielectric agrees with the results obtained by Glaser [3] for a hollow cylindrical channel in a lossy dielectric.

APPENDIX C

RAY METHOD

The allowed modes in a rectangular tunnel in a dielectric can also be determined approximately by a ray theory approach. In this method we consider a ray of the radiation that bounces from wall to wall of the tunnel making a grazing angle ϕ_1 with the side walls and ϕ_2 with the floor and roof. The E_h and E_v (1,1) modes are both defined in the ray picture by the phase relations

$$\sin \phi_1 = \frac{\lambda}{2d_1} \tag{C1}$$

$$\sin \phi_2 = \frac{\lambda}{2d_2}. \tag{C2}$$

Equations (C1) and (C2) are the conditions that the phase shift undergone by the ray is exactly 360° after successive reflections from the two side walls or from the floor and roof.

For frequencies around 1000 MHz, λ is small compared with d_1 and d_2. Therefore we can use the approximate relations

$$\phi_1 = \frac{\lambda}{2d_1} \tag{C3}$$

$$\phi_2 = \frac{\lambda}{2d_2}. \tag{C4}$$

The numbers of reflections N_1 and N_2 experienced by a ray at the vertical and horizontal walls of the tunnel, while traveling a distance z along the tunnel, are given by

$$N_1 = \frac{z\phi_1}{d_1} \tag{C5}$$

$$N_2 = \frac{z\phi_2}{d_2}. \tag{C6}$$

The attenuation factor for the ray intensity for this distance is

$$\frac{I}{I_0} = R_1^{N_1} R_2^{N_2} \tag{C7}$$

where R_1 and R_2 are the power reflectances of the vertical and horizontal surfaces at the grazing angles ϕ_1 and ϕ_2, respectively.

On combining (C3)–(C7) we find for the loss L in decibels

$$L = 5\lambda z \left(\frac{1}{d_1^2} \log_{10} \frac{1}{R_1} + \frac{1}{d_2^2} \log_{10} \frac{1}{R_2} \right). \tag{C8}$$

For the E_h mode the reflectances R_1 and R_2 of the vertical and horizontal walls, respectively, are given by the Fresnel formulas

$$R_{1Eh} = \left| \frac{K_1 \sin \phi_1 - (\sin^2 \phi_1 + K_1 - 1)^{1/2}}{K_1 \sin \phi_1 + (\sin^2 \phi_1 + K_1 - 1)^{1/2}} \right|^2 \tag{C9}$$

$$R_{2Eh} = \left| \frac{\sin \phi_2 - (\sin^2 \phi_2 + K_2 - 1)^{1/2}}{\sin \phi_2 + (\sin^2 \phi_2 + K_2 - 1)^{1/2}} \right|^2. \tag{C10}$$

For the E_v mode the corresponding formulas are

$$R_{1Ev} = \left| \frac{\sin \phi_1 - (\sin^2 \phi_1 + K_1 - 1)^{1/2}}{\sin \phi_1 + (\sin^2 \phi_1 + K_1 - 1)^{1/2}} \right|^2 \tag{C11}$$

$$R_{2Ev} = \left| \frac{K_2 \sin \phi_2 - (\sin^2 \phi_2 + K_2 - 1)^{1/2}}{K_2 \sin \phi_2 + (\sin^2 \phi_2 + K_2 - 1)^{1/2}} \right|^2. \tag{C12}$$

Table VIII gives calculated values of grazing angle, number of reflections, reflectance, and loss for the E_h mode in a 14-ft × 7-ft high-coal tunnel with $K_1 = K_2 = 10$. L_1 and L_2 are the loss rates at the side walls and at the roof and floor, respectively. The total loss L agrees very well with the E_h mode theory results shown in Fig. 2.

[3] A representative nominal value for tunnel walls in bituminous coal seams.

TABLE VIII

RAY METHOD CALCULATIONS (FOR E_h MODE)

f (MHz)	λ (ft)	ϕ_1 (deg)	ϕ_2 (deg)	N_1 (Bounces/100 ft)	N_2 (Bounces/100 ft)	R_1	R_2	L_1 (dB/100 ft)	L_2 (dB/100 ft)	L (dB/100 ft)
1000	0.984	2.0	4.0	0.25	1.00	0.62	0.90	0.51	0.41	0.92
415	2.370	4.9	9.7	0.60	2.42	0.37	0.79	3.05	2.38	5.43
200	4.918	10.1	20.1	1.25	5.02	0.068	0.62	11.40	10.17	21.57

APPENDIX D

LOSS DUE TO SURFACE ROUGHNESS

When a parallel beam of radiation of intensity I_0 strikes a rough surface at normal incidence the reflected radiation consists of a parallel beam of reduced intensity I together with a diffuse component. If the surface is a perfect reflector

$$I = I_0 \exp\left[-2\left(\frac{2\pi}{\lambda}h\right)^2\right] \tag{D1}$$

where λ is the wavelength and h is the root-mean-square roughness. For incidence at a grazing angle ϕ one may assume that the effective roughness is now $h \sin \phi$, so the loss factor becomes [6]

$$f = \exp\left[-2\left(\frac{2\pi}{\lambda}h \sin \phi\right)^2\right]. \tag{D2}$$

In the case of the dominant mode in a dielectric waveguide we can, from (C1) and (C2), write for the roughness loss factors per reflection for the vertical and horizontal walls

$$f_1 = \exp\left[-2\left(\frac{\pi h}{d_1}\right)^2\right] \tag{D3}$$

$$f_2 = \exp\left[-2\left(\frac{\pi h}{d_2}\right)^2\right]. \tag{D4}$$

The loss factor for a distance z is therefore, from C(3)–C(6)

$$f = \exp\left[-2N_1\left(\frac{\pi h}{d_1}\right)^2 - 2N_2\left(\frac{\pi h}{d_2}\right)^2\right]$$

$$\approx \exp\left[-\pi^2 h^2 \lambda\left(\frac{1}{d_1^4} + \frac{1}{d_2^4}\right)z\right]. \tag{D5}$$

The loss in dB is then

$$L_{\text{roughness}} = 4.343\pi^2 h^2 \lambda\left(\frac{1}{d_1^4} + \frac{1}{d_2^4}\right)z. \tag{D6}$$

APPENDIX E

LOSS DUE TO TILT OF TUNNEL WALLS

The effect of wall tilt can be estimated as follows. Suppose that a ray of the E_h mode encounters a portion of a side wall that is tilted through a small angle θ about a vertical axis. Then the reflected beam is rotated through an angle 2θ. This means that the electric field is changed from

$$E_x = F(x,y) \exp(-ik_3 z) \tag{E1}$$

to

$$E_x' = F(x,y) \exp[-ik_3(z \cos 2\theta + x \sin 2\theta)]. \tag{E2}$$

The power coupling factor g_1 of the disturbed field (E2) back into the mode (E1) is given by

$$g_1 = \frac{|\iint E_x \bar{E}_x' \, dx\, dy|^2}{\iint |E_x|^2 \, dx\, dy \iint |E_x'|^2 \, dx\, dy} \tag{E3}$$

where the integrations are over the cross section of the tunnel. The bar over E_x' indicates complex conjugate. Since θ is small we can replace $\cos 2\theta$ by 1 and $\sin 2\theta$ by 2θ. Then (E3) becomes

$$g_1 = \frac{|\iint |F|^2 \exp(2ik_3 x\theta) \, dx\, dy|^2}{(\iint |F|^2 \, dx\, dy)^2}. \tag{E4}$$

Instead of using the actual function $\cos k_1 x \cos k_2 y$ for F, we find it more convenient to use an equivalent Gaussian function

$$F = F_0 \exp\left[-\left(\frac{x^2}{a^2} + \frac{y^2}{b^2}\right)\right] \tag{E5}$$

and integrate over infinite limits. The result is

$$g_1 = \exp(-\tfrac{1}{2}k_3^2 a^2 \theta^2). \tag{E6}$$

Next we assume that F^2 falls to $1/e$ at the point $x = d_1/2$, $y = 0$, which is at the surface of the waveguide. Then $a^2 = 1/2d_1^2$ and

$$g_1 = \exp(-\tfrac{1}{4}k_3^2 d_1^2 \theta^2). \tag{E7}$$

Likewise, tilting of the floor or roof gives a coupling factor

$$g_2 = \exp(-\tfrac{1}{4}k_3^2 d_2^2 \theta^2). \tag{E8}$$

The loss factor for a distance z is

$$g = g_1^{N_1} g_2^{N_2} = \exp\left(-\frac{\pi^2\theta^2 z}{\lambda}\right) \tag{E9}$$

where we have replaced k_3 by k_0.

The loss in dB is therefore

$$L_{\text{tilt}} = \frac{4.343\pi^2\theta^2 z}{\lambda}. \tag{E10}$$

APPENDIX F

PROPAGATION AROUND A CORNER

A. Transmission of Diffuse Component Around a Corner

To calculate the fraction of the diffuse component in the main tunnel that goes around a corner into a cross tunnel, we use results given in graphical form by Sparrow and Cess [7] for the angle factors for diffuse radiation transfer between rectangular areas, on the assumption that the radiation in the main tunnel is perfectly diffuse. In the high-coal case of intersecting tunnels each of dimensions 14 ft by 7 ft, the angle factor between the main tunnel aperture 1 and the cross tunnel aperture 2 is

$$F_{1\to 2}(\text{high coal}) = 0.15 = -8.2\ \text{dB}. \tag{F1}$$

In the case of low-coal tunnels of dimensions 14 ft $\times$ 3.5 ft, the result is

$$F_{1\to 2}(\text{low coal}) = 0.10 = -10\ \text{dB}. \tag{F2}$$

B. Excitation of E_h Mode in Cross Tunnel by Diffuse Component in Main Tunnel

Fig. 12 depicts the geometry used for computing the degree to which the E_h mode in the main tunnel couples to the E_h mode in a cross tunnel. Diffuse radiation passing through a cross section A of the main tunnel has the angular distribution

$$dP = \frac{P_0 \cos\theta}{\pi A}\, d\Omega\, dA \tag{F3}$$

where

- dP power in element of solid angle $d\Omega$ from element of area dA,
- θ angle with normal to dA,
- P_0 total diffuse power,
- A total area of cross section.

The power entering the E_h mode in the cross tunnel is therefore

$$P = \frac{1}{2}\frac{P_0}{\pi A}\int_\Omega\int_A \cos\theta\, d\Omega\, dA \tag{F4}$$

where the integration is taken over the whole area A of the cross section and over the solid angle Ω of the mode. The factor 1/2 allows for the horizontal polarization of the mode. Ω is defined by the angles

$$\phi_1 = \frac{\lambda}{2d_1} \tag{F5}$$

$$\phi_2 = \frac{\lambda}{2d_2} \tag{F6}$$

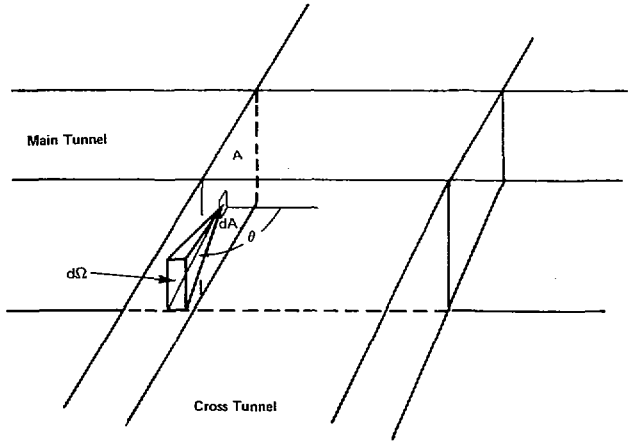

Fig. 12. Geometry for coupling to cross tunnels.

d_1 and d_2 being the horizontal and vertical dimensions of the tunnel. Therefore

$$\Omega = 2\phi_1\phi_2 = \frac{\lambda^2}{2d_1d_2}. \tag{F7}$$

Since ϕ_1 and ϕ_2 are small, the contributions of various elements dA are approximately equal since shadowing effects can be neglected. Therefore (F4) becomes

$$\begin{aligned} P &= (2\phi_2)\frac{P_0}{2\pi}\int_{\theta=\pi/2-\phi_1}^{\pi/2} \cos\theta \sin\theta\, d\theta \\ &= \frac{2\phi_2 P_0}{2\pi}\frac{1}{2}[1 - \sin^2(\pi/2 - \phi_1)] \\ &= \frac{\phi_2 P_0}{2\pi}(1 - \cos^2\phi_1) \\ &\approx \frac{\phi_2\phi_1^2 P_0}{4\pi} \\ &= \frac{\lambda P_0}{16\pi d_1^2 d_2}. \end{aligned} \tag{F8}$$

The power ratio of the E_h mode in the cross tunnel and main tunnel is

$$\frac{P_{Eh-\text{cross}}}{P_{Eh-\text{main}}} = \frac{P}{P_{Eh-\text{main}}} = \frac{P_0}{P_{Eh-\text{main}}}\frac{\lambda^3}{16\pi d_1^2 d_2} \tag{F9}$$

where P_0 is the diffuse power level in the main tunnel. This result neglects any contribution from scattering by the floor and roof of the intersection area between the two tunnels.

APPENDIX G

ANTENNA INSERTION LOSS

A half-wave dipole antenna centered at x_0, y_0 in the tunnel and oriented in the x direction is approximated by

a surface current distribution

$$\bar{K}(x,y) = \bar{i}_x I_0 \cos\left(\frac{2\pi x}{\lambda}\right) u_0(y - y_0)$$

$$\cdot\left\{u_{-1}\left[x + \left(x_0 - \frac{\lambda}{2}\right)\right] - u_{-1}\left[x - \left(x_0 + \frac{\lambda}{2}\right)\right]\right\} \quad \text{(G1)}$$

where u_0 and u_{-1} are the unit impulse and step functions.

For the case of an infinite tunnel extending to either side of the dipole, the tangential field components take on the usual form

$$\bar{H}_{\pm} = \sum_{j,k} \bar{h}_{jk} \frac{1}{Z_{0jk}} V_{\pm jk} \exp(\pm\gamma_{jk} z) \quad \text{(G2)}$$

$$\bar{E}_{\pm} = \sum_{j,k} \bar{e}_{jk} V_{\pm jk} \exp(\pm\gamma_{jk} z) \quad \text{(G3)}$$

$$\bar{h}_{jk} = \bar{h}_{0jk} \cos k_1 x \cos k_2 y \quad \text{(G4)}$$

$$\bar{e}_{jk} = \bar{e}_{0jk} \cos k_1 x \cos k_2 y \quad \text{(G5)}$$

where Z_{ojk}, $V_{\pm jk}$, $\bar{h}_{ojk}$, and $\bar{e}_{ojk}$ are the characteristic impedance, + and − wave voltage coefficients, and normalization constants, respectively, for each waveguide mode. By matching the tangential boundary conditions over the cross section containing the dipole and selecting the dominant (1,1) E_h mode contribution by using the mode orthogonality properties, we obtain

$$V_{+,1,1} = V_{-,1,1} \quad \text{(G6)}$$

$$V_{+,1,1} = -\frac{Z_{0,1,1}}{2} \int_x \int_y (\bar{i}_z \times \bar{K}(x,y)) \cdot \bar{h}_{1,1}(x,y)\, dx\, dy. \quad \text{(G7)}$$

Carrying out the integration we get

$$V_{+,1,1} = \frac{I_0 \lambda}{2\pi} Z_{0,1,1} h_{0,1,1} \cos k_1 x_0 \cos k_2 y_0. \quad \text{(G8)}$$

The total power coupled into the dominant (1,1) E_h waveguide mode propagating in both tunnel directions, to the left and to the right of the dipole, is

$$P_{\text{mode}} = \frac{|V_{+,1,1}|^2}{Z_{0,1,1}}. \quad \text{(G9)}$$

The power radiated by the dipole is

$$P_{\text{dipole}} = \tfrac{1}{2} I_0^2 R_r \quad \text{(G10)}$$

where R_r is the dipole radiation resistance. The desired coupling factor C is the fraction of the dipole radiated power that is coupled to the (1,1) E_h mode propagating in one of the tunnel directions for a half-wave dipole; C is given by

$$C = \frac{\frac{1}{2}P_{\text{mode}}}{P_{\text{dipole}}} = \frac{\lambda^2}{4\pi^2} \frac{Z_{0,1,1}}{R_r} h_{0,1,1}^2 \cos^2 k_1 x_0 \cos^2 k_2 y_0. \quad \text{(G11)}$$

When the wavelength is small compared with the tunnel cross-sectional dimensions, the cosine factors are approximately zero at the tunnel walls, so that $k_1 \cong \pi/d_1$, $k_2 \cong \pi/d_2$ and $h_{0,1,1} \cong 2/(d_1 d_2)^{1/2}$. Then (G11) becomes

$$C = \frac{Z_{0,1,1}\lambda^2}{\pi^2 R_r d_1 d_2} \cos^2 \frac{\pi x_0}{d_1} \cos^2 \frac{\pi y_0}{d_2}. \quad \text{(G12)}$$

REFERENCES

[1] A. G. Emslie, R. L. Lagace, and P. F. Strong, "Theory of the propagation of UHF radio waves in coal mine tunnels," in *Proc. Through-the-Earth Electromagnetics Workshop*, Colorado School of Mines, Golden, Colo., Aug. 15–17, 1973, available from Nat. Tech. Inform. Service, Alexandria, Va.

[2] E. A. J. Marcatili and R. A. Schmeltzer, "Hollow metallic and dielectric waveguides for long distance optical transmission and lasers," *Bell Syst. Tech. J.*, vol. 43, p. 1783, 1964.

[3] J. I. Glaser, "Attenuation and guidance of modes in hollow dielectric waveguides," *IEEE Trans. Microwave Theory Tech.* (Corresp.), vol. MTT-17, pp. 173–174, Mar. 1969; and M.I.T., Cambridge, Mass., Ph.D. thesis, Dep. Elec. Eng., "Low-loss waves in hollow dielectric tubes," Feb. 1967.

[4] A. E. Goddard, "Radio propagation measurements in coal mines at UHF and VHF," in *Proc. Through-the-Earth Electromagnetics Workshop*, Colorado School of Mines, Golden, Colo., Aug. 15–17, 1973, available from Nat. Tech. Inform. Service, Alexandria, Va.

[5] Bureau of Mines Information Circular/1974, IC-8635, "Mine communications," *Proc. Bureau of Mines Technology Transfer Seminar*, Bruceton, Pa., Mar. 21–22, 1973.

[6] P. Beckmann and A. Spizzichino, *The Scattering of Electromagnetic Waves from Rough Surfaces*. New York: Macmillan, 1963, p. 81, eq. (6).

[7] E. M. Sparrow and R. D. Cess, *Radiation Heat Transfer*. Belmont, Calif.: Wadsworth, 1966, App. A.